sion process indicate that radiation can occur at both the fundamental and the second harmonic of the plasma frequency (*8*). However, the theories have not been definitive in resolving the question of which process dominates (*9*). For the event shown, the second harmonic interpretation of the radio emission is in much better conformity with the interpolated solar wind densities. If, however, emission occurs at the fundamental, one must explain why the radiation occurs preferentially in density-enhanced inhomogeneities.

From the measured drift time from one frequency to another we can determine the speed of the exciter particles. These data are shown in Fig. 2B. The values used in the upper curve were obtained from the burst onset times corresponding to the fastest particles. The peak times were used in the lower curve, which corresponds more closely to the average velocity in the exciter. Both curves indicate an apparent deceleration of the exciter by a factor of about 2 over distances out to 1 A.U.; this indicates a 75 percent loss in energy.

The measurement of radio arrival directions is a method for obtaining information about remote portions of the interplanetary medium. Additional information would be expected from a study of many bursts of this type. The simultaneous data provided by a second spinning spacecraft could be of great value in defining the actual radio positions.

J. FAINBERG
LARRY G. EVANS
R. G. STONE

Radio Astronomy Branch, Laboratory for Extraterrestrial Physics, NASA–Goddard Space Flight Center, Greenbelt, Maryland 20771

References and Notes

1. E. N. Parker, *Astrophys. J.* **128**, 664 (1958); *Interplanetary Dynamical Processes* (Interscience, New York, 1963), pp. 41–72.
2. J. M. Wilcox, *Science* **152**, 161 (1966).
3. R. P. Lin and K. A. Anderson, *Solar Phys.* **1**, 446 (1967).
4. M. R. Kundu, *Solar Radio Astronomy* (Interscience, New York, 1965), pp. 50–64.
5. J. Fainberg and R. G. Stone, *Solar Phys.* **17**, 392 (1971).
6. R. Michard, *Ann. Astrophys.* **17**, 429 (1954); D. E. Blackwell, *Mon. Not. Roy. Astron. Soc.* **116**, 57 (1956); D. E. Blackwell and A. D. Petford, *ibid.* **131**, 399 (1966).
7. A. J. Hundhausen, *Space Sci. Rev.* **8**, 690 (1968).
8. V. L. Ginzburg and V. V. Zheleznyakov, *Sov. Astron. AJ* **2**, 653 (1958); S. A. Kaplan and V. N. Tsytovich, *ibid.* **11**, 1956 (1968); D. F. Smith, *Advan. Astron. Astrophys.* **7**, 147 (1970).
9. V. V. Zheleznyakov and V. V. Zaitsev, *Sov. Astron. AJ* **14**, 47, 250 (1970).
10. L.G.E. is a NAS-NRC postdoctoral resident research associate.

20 July 1972

Mercury: Surface Composition from the Reflection Spectrum

Abstract. *The reflection spectrum for the integral disk of the planet Mercury was measured and was found to have a constant positive slope from 0.32 to 1.05 micrometers, except for absorption features in the infrared. The reflectivity curve matches closely the curve for the lunar upland and mare regions. Thus, the surface of Mercury is probably covered with a lunar-like soil rich in dark glasses of high iron and titanium content. Pyroxene is probably the dominant mafic mineral.*

The spectral reflectivity of the integral disk of Mercury was determined at two different times for the spectral region 0.32 to 1.05 μm. The first measurements were made on the afternoon and evening of 25 December 1969 by using the 60-inch (152.4 cm) telescope of the Cerro Tololo Interamerican Observatory, La Serena, Chile. A dual-beam photometer was used in a sky-subtraction mode with a cooled S-1 photomultiplier tube (ITT model FW-130) and an analog synchronous detection data system (*1*). A set of 22 narrow-band interference filters (200 to 500 Å bandwidth) spaced evenly across the spectral region was used to scan the spectrum (*2*). The star 29 Psc was observed from near twilight until it reached a zenith angle greater than that for the last of the four observations of Mercury. The phase angle of Mercury was 70°.

The second set of measurements was obtained during evening twilight on 12 March 1972 by using the 36-inch (91.44 cm) number 2 telescope of the Kitt Peak National Observatory, Kitt Peak, Arizona. The dual-beam photometer was used in the same mode as in the earlier measurements, with the same photomultiplier tube and filter set. A pulse-counting digital data system was used. The integral disk of Mercury was measured six times alternately with the star ξ^2 Ceti. The phase angle of Mercury was 84°.

Both sets of data were reduced in the same way. Curves of intensity plotted against air mass were prepared for each object, for each filter. For each measurement of Mercury, the ratios of the intensities for Mercury to those for the star at equal air mass for each filter were calculated. The Mercury/star intensity ratios were multiplied by star/sun flux intensity ratios (*2*) to produce reflectivities at each effective filter wavelength (*2*). The values were scaled to unity at 0.564 μm to produce a normalized spectral reflectivity curve for Mercury for each night's observations (Fig. 1). The flux values and reflectivities are available from the authors.

The two measurements shown in

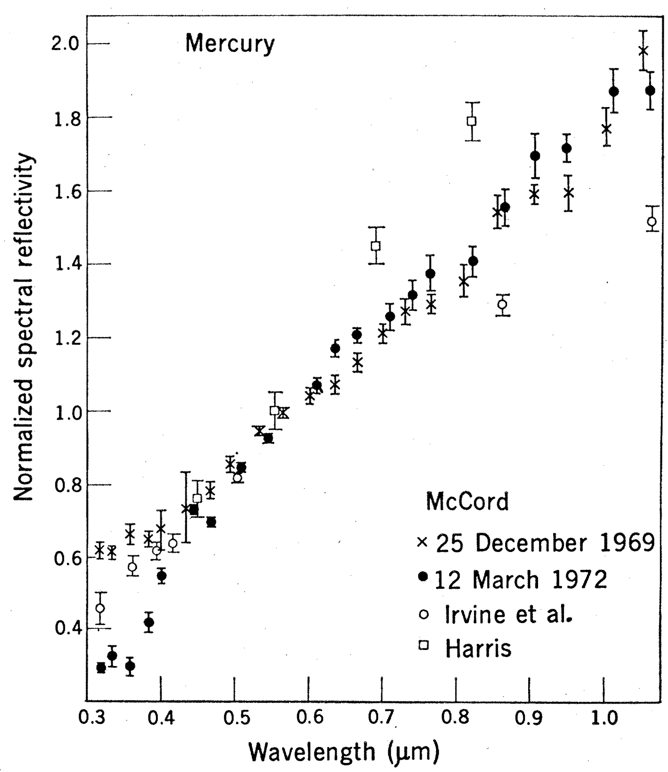

Fig. 1. Spectral reflectivity of the integral disk of Mercury scaled to unity at 0.564 μm for each of two observations. The wavelength position for each point is the same for both data sets, but the 1972 points (filled circles) are offset to the right from the 1969 points (crosses) to make the error bar visible. Also shown are the results of Irvine *et al.* (*3*) and Harris (*4*).

Fig. 1 agree within the error bars except for the ultraviolet spectral region. We cannot identify any observational systematic error to explain the disagreement in the ultraviolet, although this spectral region is the most difficult in which to work.

The flux received from Mercury above the earth's atmosphere was calculated for the Kitt Peak data and is available from the authors. The albedo on Mercury can be calculated from these data.

Values of the spectral reflectivity of the integral disk of Mercury obtained by Irvine *et al.* (*3*) and Harris (*4*) are shown in Fig. 1 along with the results of the two new measurements described here. All the measurements show that there is an increase in reflectance with wavelength, but the slope of the curve varies among the data sets. The reason for this difference is unknown, but phase angle effects apparently are not responsible. Only the most recent data set has sufficient spectral resolution to resolve absorption features. This curve does show two weak features in the infrared, one of which we interpret as a shallow absorption band commonly found for silicate minerals. The short-wavelength feature does not correspond to any known absorption and thus is somewhat suspect.

The most recent integral spectral reflectivity curve for Mercury is compared in Fig. 2 to the spectral reflectivity curves for four different areas of the moon. The moon exhibits different types of reflectivity curves for different types of terrain, that is, maria, uplands, bright mare craters, and bright upland craters (*5*). Most of the lunar surface is covered by mare and upland material and thus, if the moon were viewed integrally as Mercury was, the properties observed would be those of these two types of area. The reflectivity curve for Mercury is quite similar to that for the lunar upland and mare material, and thus the integral spectral reflectivity of Mercury is quite similar to that of the integral moon.

The lunar spectral reflectivity curves for mare and upland material, in the spectral region shown in Fig. 1, have two major features: (i) a uniform positive slope, and (ii) a shallow absorption band near 0.95 μm. A study of lunar surface material has shown that the slope of the spectral reflectivity curve for the moon is controlled by the glass rich in titanium and iron in the lunar soil and that the absorption band at 0.95 μm is mainly an expression of the mineral pyroxene in the soil (*6*).

In slope and shape, the lunar spectral reflectivity curve is not matched by the curves for silicate or other common minerals, including the metals and metal oxides such as ilmenite ($FeTiO_3$) and magnetite (Fe_3O_4); it seems to be matched uniquely by the curves for the dark silicate glasses that are rich in titanium and iron. These glasses are created in the lunar soil by meteoroid impact, which vitrifies a portion of the impacted material. Iron and titanium ions must be present in the primary surface material in order for the dark glasses to be created (*6*). The principal source of these ions on the moon is the mineral ilmenite.

Absorption bands in the spectral region 0.90 to 1.00 μm are common for pyroxene minerals (*7, 8*). An increase in the wavelength of the absorption band is related to an increase in the calcium content and Fe/Mg ratio of the mineral. Also, the mineral olivine, which is often present in igneous rocks containing pyroxene, has an absorption band located just beyond 1.0 μm. The olivine band can combine with the pyroxene band, when both minerals are present in the sample, to produce a combination band with the band position shifted longward of that for pyroxene alone. The exact position of the absorption band in the lunar samples is determined primarily by the calcium content of the pyroxene and, in only a few rocks, by the presence of small amounts of olivine. Band positions in the spectra of the lunar soils are an expression of pyroxene composition only. The telescopic lunar spectra have been shown to be controlled by the soil alone, with apparently little contribution from rocks and breccias (*6, 8*).

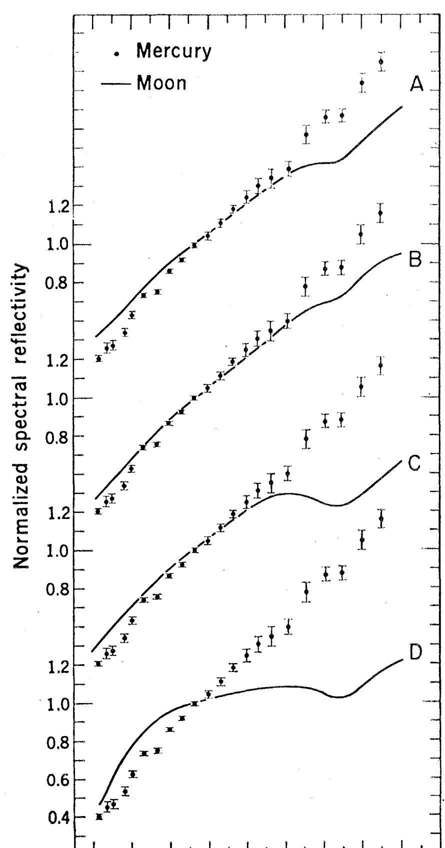

Fig. 2. The spectral reflectivity of the integral disk of Mercury (average of 1969 and 1972 results) scaled to unity at 0.564 μm (filled circles) is compared with the reflection spectra for four different lunar terrains: *A*, uplands; *B*, maria; *C*, bright upland craters; *D*, mare bright craters.

The close similarity of the features in the reflection spectra of Mercury and the moon strongly suggests a similarity in the mineralogy and composition of their soils. Titanium-rich and iron-rich glasses, presumably created by impact, should be common on Mercury. This is supported by the fact that Mercury has a low albedo similar to that for the integral moon. The weak 0.95-μm absorption band in the spectra of Mercury suggests that pyroxene is the major mafic mineral responsible for the band. The presence of dark glasses requires that titanium-rich and iron-rich minerals such as ilmenite were there to be vitrified. The 0.95-μm band suggests that some crystalline pyroxenes still remain.

THOMAS B. MCCORD

Planetary Astronomy Laboratory, Department of Earth and Planetary Sciences, Massachusetts Institute of Technology, Cambridge 02139

JOHN B. ADAMS

West Indies Laboratory, Fairleigh Dickinson University, St. Croix, Virgin Islands

References and Notes

1. T. B. McCord, *Appl. Opt.* **7**, 475 (1968).
2. See T. B. McCord and J. A. Westphal [*Astrophys. J.* **168**, 141 (1971)] for filter characteristics.
3. W. M. Irvine, T. Simon, D. Menzel, C. Pikoos, A. T. Young, *Astron. J.* **73**, 807 (1968).
4. D. L. Harris, in *Planets and Satellites*, G. P. Kuiper and B. M. Middlehurst, Eds. (Univ. of Chicago Press, Chicago, 1961), vol. 3, p. 307.
5. T. B. McCord, M. P. Charette, T. V. Johnson, L. A. Lebofsky, C. Pieters, J. B. Adams, *J. Geophys. Res.* **77**, 1349 (1972).
6. J. B. Adams and T. B. McCord, *Science* **171**, 567 (1971); in *Proceedings of the Second Lunar Science Conference*, A. A. Levinson, Ed. (M.I.T. Press, Cambridge, Mass., 1971), vol. 3, p. 2138.
7. R. G. Burns, *Mineralogical Applications of Crystal Field Theory* (Cambridge Univ. Press,

Cambridge, England, 1970); J. B. Adams, in preparation.
8. J. B. Adams and T. B. McCord, in *Proceedings of the Apollo 11 Lunar Science Conference*, A. A. Levinson, Ed. (Pergamon, New York, 1970), vol. 3, p. 1937.
9. Several students, particularly J. Elias, J. Kunin, and M. Keyes, were extremely helpful with the data reduction. Supported by NASA grant NGR 22-009-350. T.B.M. is a visiting astronomer at Cerro Tololo Inter-American Observatory and Kitt Peak National Observatory, which are operated by the Association of Universities for Research in Astronomy, Inc., under contract with the National Science Foundation. Contribution No. 51 of the Planetary Astronomy Laboratory.

14 August 1972; revised 25 September 1972 ■

Orbit-Orbit Resonance Capture in the Solar System

Abstract. *A realistic model involving mutual gravitation and tidal dissipation for the first time provides a detailed explanation for satellite orbit-orbit resonance capture. Although applying directly only to Saturn's satellites Titan and Hyperion, the model reveals general principles of resonance capture, evolution, and stability which seem applicable to other orbit-orbit resonances in the solar system.*

Many pairs of natural satellites have orbits that are locked in stable resonances: Their gravitational interaction maintains the low-order commensurability of their orbital periods. The relatively large number of such commensurabilities in the solar system has led many to believe that satellites have evolved into resonances from orbits with originally incommensurate periods (*1*). But the mechanism of capture into resonance has never been described. In this report, we discuss a simple theoretical model which demonstrates that tidal evolution can cause certain satellite pairs to be inevitably captured into orbit-orbit resonance.

The model was inspired by Saturn's satellites Titan and Hyperion. The average ratio of their respective orbital periods, measured relative to Hyperion's major axis, is 3/4. The longitude of their conjunction librates about Hyperion's longitude of apocenter (see Fig. 1). Conventionally, this resonance is described by using a "resonance variable," ϕ, defined as $4\lambda_2 - 3\lambda_1 - \tilde{\omega}_2$, where λ is the mean longitude and $\tilde{\omega}$ the longitude of pericenter, with the subscripts 1 and 2 referring to Titan and Hyperion, respectively. In this case, ϕ librates about 180° with an amplitude of 36° and a period of 640 days. A simple model can be useful because of Titan's larger mass (10^3 times that of Hyperion) and smaller orbital eccentricity (0.03 compared to Hyperion's 0.10). The slight asymmetry of Titan's orbit, represented by its eccentricity, has no effect on the qualitative aspects of the resonance capture mechanism.

Our model consists of a large planet of mass M and two satellites in coplanar orbits. The inner satellite, of mass m_1, has a circular orbit with a period constantly increasing due to tidal friction (*1*). The outer satellite, of mass m_2, is too small to perturb m_1 or to raise a significant tide on M ($M \gg m_1 \gg m_2$). The eccentricity of the outer orbit, e_2, is taken to be small enough to permit a valid first-order analysis.

An analytical approach is more fruitful than a numerical one because it leads to a simple physical interpretation. The analysis is outlined below with the emphasis placed on the qualitative mechanism of capture (*2*).

The behavior of the resonance variable, ϕ, may be deduced from Lagrange's equations for the variation of orbital elements. The disturbing function that represents the gravitational effects of m_1 on m_2 in these equations has a well-known trigonometric series expansion (*3*). Using this expansion and ignoring terms with short-period arguments, we find

$$\frac{d\phi}{dt} = 4n - 3 - \frac{1}{2e_2}\left(\frac{m_1}{M}\right)F(n)\cos\phi \quad (1)$$

where t is the time (in units of the instantaneous period of m_1), n (which is less than 1) is the ratio of the satellites' orbital periods measured relative to an inertial reference frame, and the function $F(n)$ is a dimensionless coefficient of order unity found from the expanded disturbing function. Similarly, the other variables, n and e_2, satisfy:

$$\frac{de_2}{dt} = -\frac{1}{2}\left(\frac{m_1}{M}\right)F(n)\sin\phi \quad (2)$$

$$\frac{dn}{dt} = 6e_2\left(\frac{m_1}{M}\right)nF(n)\sin\phi - n\beta \quad (3)$$

where $\beta < 0$ represents the rate of increase in the period of m_1 due to tidal friction.

If n were constant, the solutions of Eqs. 1 and 2 would yield circular trajectories in the e_2, ϕ polar coordinate plane (see Fig. 2). Circle B in this figure represents libration of ϕ about 180°; circle A depicts circulation through 360°. The centers of both circles have ordinate values $e_2\sin\phi$ equal to 0, whereas the abscissas $e_2\cos\phi$ are approximately proportional to $(n - 3/4)^{-1}$.

Now consider circulation with n less than 3/4 but gradually increasing due to tidal evolution, and with e_2 much less than 1. The center of the corresponding circular trajectory in Fig. 2 will then move leftward, toward a state of libration. As this evolution continues beyond circle B, e_2 increases, causing the first term on the right side of Eq. 3 to become significant. During the course of a single libration, n therefore varies considerably so that the instantaneous center of curvature of the trajectory moves back and forth on the axis, yielding "bean-shaped" trajectories such as C and D in Fig. 2. For trajectory D, the value of n actually becomes greater than 3/4, causing the center of curvature to pass to a positive abscissa for part of the libration cycle.

The gradual evolution of e_2, ϕ trajectories from A to D describes a solution of Eqs. 1 to 3. This evolution begins with a typical nonresonant system in which ϕ circulates, n is not yet near a ratio of small integers, and e_2 is small. The system then evolves to a state similar to the present Titan-Hyperion configuration in which ϕ librates, n oscillates about 3/4, and e_2 is relatively large. Moreover, this mechanism permits capture of ϕ into libration only about 180°. Libration about 0° is possible for small values of e_2 and is represented by the circular trajectory E in Fig. 2. But tidal evolution destroys such a libration, since as n increases the center of the circle drifts leftward until a state of circulation is reached.

Although here we have presented only a heuristic discussion, a rigorous approach has confirmed these results. Specifically, an analytical solution was found for the trajectories for β equal to 0, and the tidal evolution was then incorporated by a technique of variation of parameters (*2*).

To further clarify the physical basis of the capture mechanism and the maintenance of the resulting resonance, we may discuss this model from a different point of view. We first consider qualitatively the stability of the resonance for β equal to 0 and for e_2 sufficiently high that the longitude of Hyperion's major axis is essentially constant (its variation is inversely pro-